ELSEVIER

PII: S0021-9290(97)00092-4

J. Biomechanics, Vol. 30, Nos. 11/12, pp. 1115–1121, 1997
© 1997 Elsevier Science Ltd. All rights reserved
Printed in Great Britain
0021-9290/97 $17.00 + .00

CONSTITUTIVE MODELLING OF BRAIN TISSUE: EXPERIMENT AND THEORY

Karol Miller* and Kiyoyuki Chinzei†

*Department of Mechanical and Materials Engineering, The University of Western Australia, Nedlands/Perth, WA 6907, Australia; and †Biomechanics Division, Mechanical Engineering Laboratory, MITI, Namiki 1-2, Tsukuba, Ibaraki, 305 Japan

Abstract—Recent developments in computer-integrated and robot-aided surgery—in particular, the emergence of automatic surgical tools and robots—as well as advances in virtual reality techniques, call for closer examination of the mechanical properties of very soft tissues (such as brain, liver, kidney, etc.). The ultimate goal of our research into the biomechanics of these tissues is the development of corresponding, realistic mathematical models. This paper contains experimental results of *in vitro*, uniaxial, unconfined compression of swine brain tissue and discusses a single-phase, non-linear, viscoelastic tissue model. The experimental results obtained for three loading velocities, ranging over five orders of magnitude, are presented. The applied strain rates have been much lower than those applied in previous studies, focused on injury modelling. The stress–strain curves are concave upward for all compression rates containing no linear portion from which a meaningful elastic modulus might be determined. The tissue response stiffened as the loading speed increased, indicating a strong stress–strain rate dependence. The use of the single-phase model is recommended for applications in registration, surgical operation planning and training systems as well as a control system of an image-guided surgical robot. The material constants for the brain tissue are evaluated. Agreement between the proposed theoretical model and experiment is good for compression levels reaching 30% and for loading velocities varying over five orders of magnitude. © 1997 Elsevier Science Ltd. All rights reserved

Keywords: Brain tissue; Mechanical properties; Mathematical modelling; Compression experiment.

INTRODUCTION

Mechanical properties of living tissues form a central subject in Biomechanics. In particular, the properties of the muscular-skeletal system, skin, lungs, blood and blood vessels have attracted much attention, e.g. see Borowski *et al.* (1992), Fung (1981), Gallagher *et al.* (1982), Mow *et al.* (1993), Schmid-Schonbein *et al.* (1986) and references cited therein. The properties of 'very' soft tissues, which do not bear mechanical loads (such as brain, liver, kidney, etc.), have not been so thoroughly investigated.

However, recent developments in robotics technology, especially the emergence of automatic surgical tools and robots (e.g. Brett *et al.*, 1995) as well as advances in virtual reality techniques (Burdea, 1996), call for closer examination of the mechanical properties of these tissues. Mathematical models of brain tissue mechanical properties may find applications, e.g. in a surgical robot control system, where the prediction of deformation is needed (Miller and Chinzei, 1995a, b), surgical operation planning and surgeon training systems based on the virtual reality techniques (Burdea, 1996 and references cited therein), where *force feedback* is needed, and *registration* (Lavallée, 1995), where knowledge of local deformation is required.

The reported experimental data on the mechanical properties of brain tissue are limited. Ommaya (1968) described mammalian brain as a 'soft, yielding structure, not as stiff as a gel nor as plastic as a paste'. Walsh and Schettini (1984) and Sahay *et al.* (1992) tried to establish elastic parameters of brain tissues by measuring induced changes in intra-cranial pressure. The experimental data, which might be used to determine constitutive relations for brain tissue, was reported in Estes and McElhaney (1970) and Galford and McElhaney (1970). The objective of those papers was providing data for head injury modelling (for discussion see Voo *et al.*, 1996), so that the investigated strain rates were much higher than those in our paper. Based on these experimental results, Pamidi and Advani (1978), and Mendis *et al.* (1995) proposed non-linear constitutive relations for human brain tissue. The work by Mendis *et al.* is discussed in Discussion and Conclusion.

In this paper we attempt to prove, that non-linear viscoelastic model, based on the strain energy function in polynomial form with time-dependent coefficients, is suitable for description of brain tissue deformation behaviour under compression, at low strain rates, typical for surgical procedures.

UNCONFINED COMPRESSION EXPERIMENT OF SWINE BRAIN TISSUE

Specimen preparation

Twelve brains from six-month old swines were collected from a slaughter house. Pigs were terminated according to standard slaughtering procedure and the samples were taken as a by-product. Specimens were not frozen at any time during the procedure. Brain weights ranged between 92.5 and 101.5 g, close to the weight of a healthy adult swine (Kumagaya and Namioka, 1987). After being removed from the dura, each brain was

Received in final form 1 *August* 1997.
*Address correspondence to: Dr K. Miller, Department of Mechanical and Materials Engineering, The University of Western Australia, Nedlands/Perth, WA 6907, Australia.

stored in physiological solution at 5°C. Usually, transportation of brains and sample preparation took one night before experiments.

Cylindrical samples of diameter ~30 mm and height ~13 mm were cut. Steel pipe (30 mm diameter) with sharp edges was used to cut the samples. The faces of the cylindrical brain specimens were smoothed manually, using a surgical scalpel. Four samples were taken from the frontal and posterial portions of the Sylvian fissure of each hemisphere for each swine brain. The ventricle surface and the arachnoid membrane formed the top and bottom faces of the sample cylinder. Thus, the arachnoid membrane and the structure of the sulci remained as parts of each specimen.

Brain tissue is very soft and adheres upon contacting almost any material. Consequently, it was very difficult to obtain an exact cylindrical shape. Usually, the diameters of opposite faces of the sample differed by approximately 3–4 mm.

Experimental set-up

Uniaxial unconfined compression of swine brain tissue was performed in a testing stand shown in Fig. 1. This particular geometry was dictated by the simplifying assumptions, underlying the development of the analytical solution for stresses (see below, Brain as a Visco-Elastic Single-Phase Continuum), used to analyse the experimental data.

The main testing apparatus was a UTM-10T (Orientec Co.) tensile stress machine. Its load cell allowed measurement of compressive force in the range 0.5–9.0 N for loading velocities between 0.005 and 500 mm min^{-1}. The vertical displacement [along z-axis in Fig. 1(b)] was measured by a micrometer with electric analog output. An important part of the experiment was the measurement of the radial displacement by a laser distance meter LB-02/LB-62 (Keyence Corp.). This measurement was intended for determining the level of tissue compressibility as well as the beginning of the loading phase of the experiment. The experiment was documented by automatically taking CCD camera images. The images were used to ensure that during the loading phase, samples had uniformly expanded in radial direction as well as that upper or lower faces of the specimen did not stick to the moving platen or support.

Experimental protocol

Cylindrical samples of tissue were axially compressed between two impermeable platens. As a result of brain tissue delicacy and adhesiveness, no pre-conditioning was performed. Only one loading cycle was executed on each sample.

To diminish the effects of friction between platens and a sample, polytetrafluoroethylene (PTFE) sheets were attached to the surfaces of the supporting base and movable platen. During overnight tests, to avoid drying of the specimen, the sample was surrounded by wet lignin and covered by a plastic shield. The tests were performed at room temperature (~22°C). At the end of the procedure no signs of dehydration were observed.

The movement of the platen began about 1 mm above the sample. Care was taken to avoid touching the specimen by the platen before starting compression as the

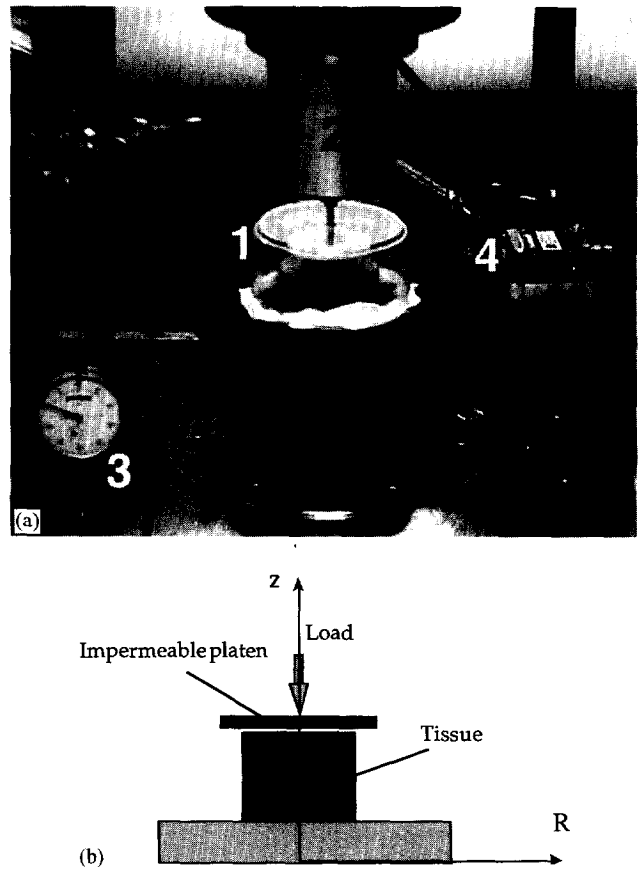

Fig. 1. Experimental setup. (a) General view with components: 1—specimen and the loading platens, 2—load cell to measure axial force, 3—micrometer to measure axial displacement, 4—laser to measure radial displacement. (b) Layout with coordinate axes.

sample tended to adhere to the platen and change shape. The start of the loading phase was indicated by the first non-zero reading of the radial displacement by laser distance meter. This method appears to be more reliable than previously used first non-zero readings of the force sensor (Estes and McElhaney, 1970), because the forces at low compression levels are very small. The end of the loading phase was indicated by the point of equalising of the reading of the micrometer measuring the vertical displacement.

Results

In the paper only the results obtained for the loading phase are discussed. The measurements for the following three loading velocities are presented:

- fast: 500 mm min^{-1}—the fastest loading speed possible with our equipment—corresponding to the strain rate of about 0.64 s^{-1};
- medium: 5 mm min^{-1}, corresponding to the strain rate of about 0.64×10^{-2} s^{-1}, and
- slow: 0.005 mm min^{-1}, corresponding to the strain rate of about 0.64×10^{-5} s^{-1}.

In each test the moving platen stopped after compressing the specimen by about 4.5 mm. Twelve fast, 13 medium speed and six slow tests were performed. Each sample was tested once only. The number of slow tests was limited because after each tissue delivery (usually two brains) only one overnight test could be performed.

To assess the repeatability of measurements, the Lagrange stresses (vertical force divided by initial cross-sectional area) versus time for each loading velocity are presented in Fig. 2 and standard deviation bars are included in Fig. 3. The coefficient of variation (standard deviation divided by the mean) for slow and medium speed tests was approximately constant and equal to 0.2 and 0.3, respectively. The coefficient of variation for fast test varied between 0.18 and 0.29. These values are significantly lower than 0.5—the value estimated from Figs. 3–6 in Estes and McElhaney (1970)—suggesting that the repeatability of experiments is significantly better than that obtained by previous researchers. The results are affected by variations between tissue samples taken from 12 swines, inherent for biological materials, and errors in estimation of sample cross-sectional area, due to deviations from cylindrical shape (up to 4%). The errors of force and displacement measurements are insignificant (not more than 0.1% of maximum force and displacement).

Figure 3 shows the relationship between the Lagrange stress and true strain [$\varepsilon = \ln \lambda_z$, where λ_z is a stretch in vertical direction, Fig. 1(b)] for three loading velocities. The standard deviation of the measurements and the theoretical predictions are indicated. The stress–strain curves are concave upward for all compression rates containing no linear portion from which a meaningful elastic modulus could be determined. The tissue response stiffened with the increasing loading speed, indicating a strong stress–strain rate dependence. The results shown in Fig. 3 are in general agreement with those published in Estes and McElhaney (1970). The results obtained for $\dot{\lambda} = 0.64\ s^{-1}$ are very close to those reported by Estes and McElhaney, for $\dot{\lambda} = 0.8\ s^{-1}$. It needs to be pointed out here that for slower strain rates there is no other data available for comparisons.

The measurement of the radial displacement was not successful due to the laser distance meter sensitivity to the reflection angle and sample colour changes. The repeatability was not sufficient to state with confidence the value of the finite deformation analog of the Poison's ratio of swine brain tissue. As it was not possible to challenge the common assumption of tissue incompressibility (e.g. Estes and McElhaney, 1970; Mendis *et al.*, 1995; Pamidi and Advani, 1978; Ruan *et al.*, 1994, Voo *et al.*, 1996), in the theoretical part of the paper, the incompressibility of brain tissue is assumed. The laser distance meter was still very useful in determination of the beginning of sample lateral expansion, which was considered as the start of the loading phase.

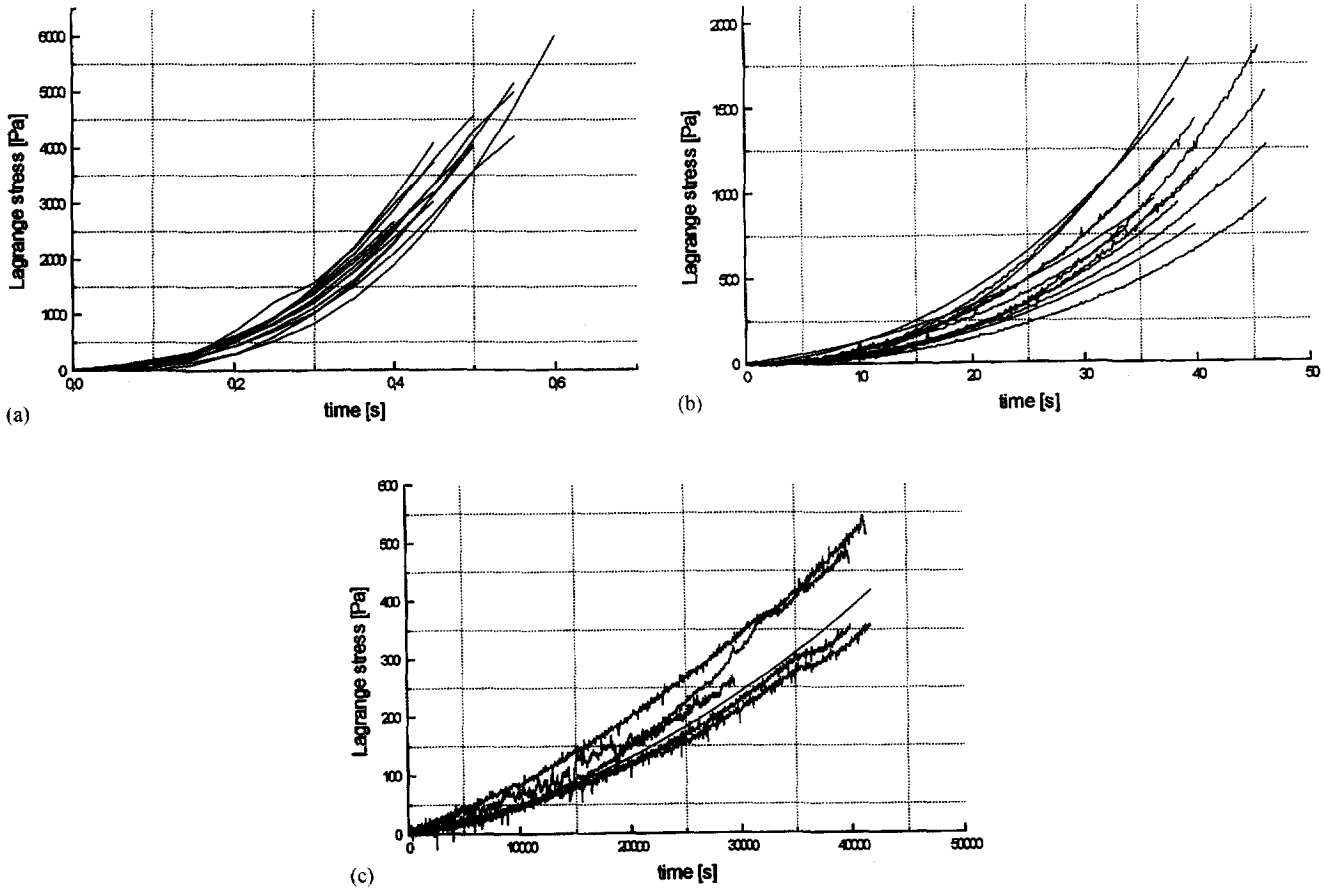

Fig. 2. Repeatability of measurements: (a) loading speed 500 mm min^{-1}, corresponding to the strain rate of about 0.64 s^{-1}; (b) loading speed 5 mm min^{-1}, corresponding to the strain rate of about 0.64×10^{-2} s^{-1}; (c) loading speed 0.005 mm min^{-1}, corresponding to the strain rate of about 0.64×10^{-5} s^{-1}.

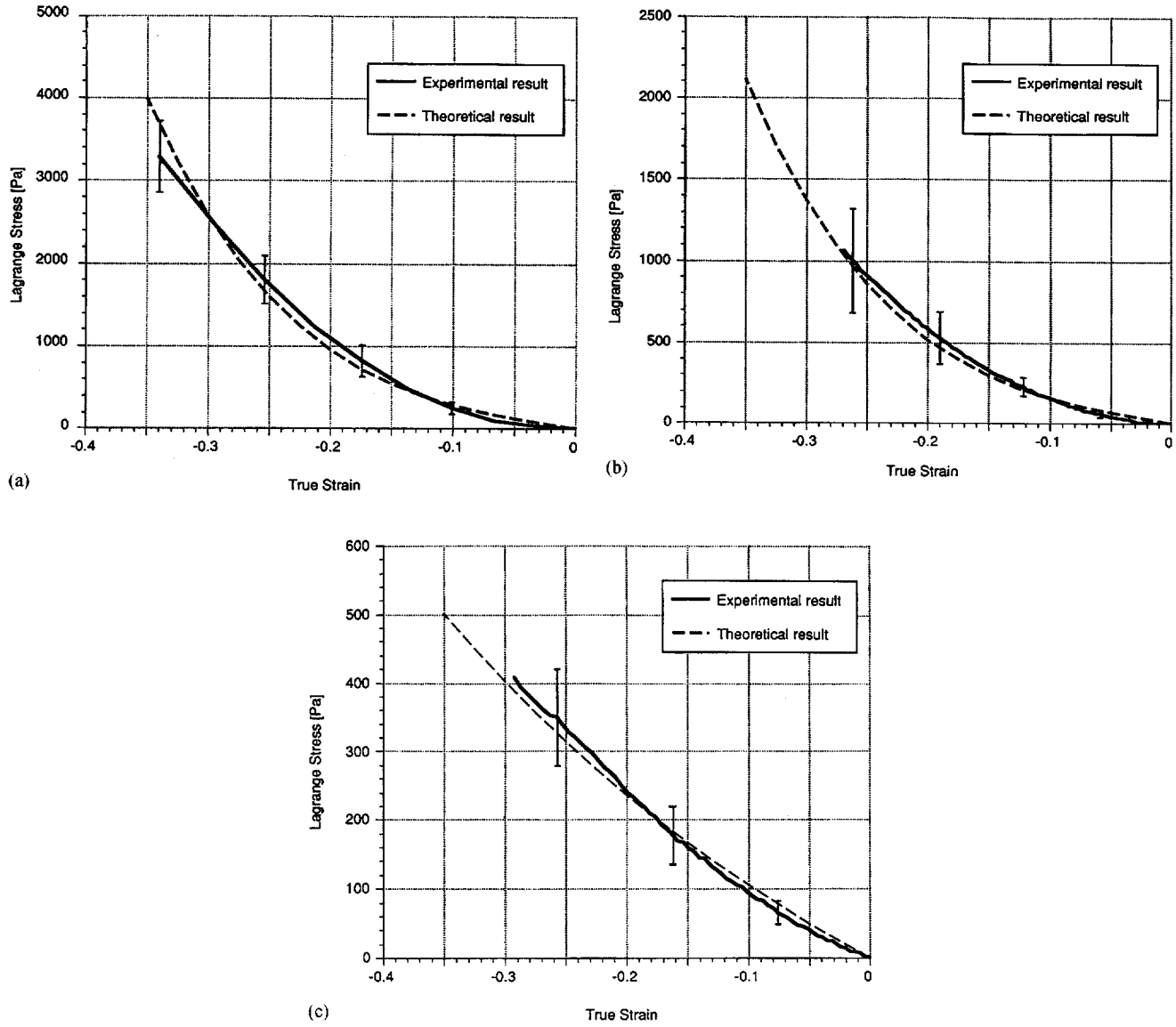

Fig. 3. Lagrange stress–true strain relations for swine brain tissue, experimental and theoretical results. Error bars indicate standard deviation. (a) loading speed 500 mm min^{-1}, corresponding to the strain rate of about 0.64 s^{-1}; (b) loading speed 5 mm min^{-1}, corresponding to the strain rate of about 0.64×10^{-2} s^{-1}; (c) loading speed 0.005 mm min^{-1}, corresponding to the strain rate of about 0.64×10^{-5} s^{-1}.

BRAIN AS A VISCOELASTIC SINGLE-PHASE CONTINUUM

Modelling of finite deformation non-linear tissue behaviour

To begin the modelling of non-linear stress–strain dependence, the strain energy function of the following form is used:

$$W = \sum_{i+j=1}^{N} C_{ij}(J_1 - 3)^i (J_2 - 3)^j, \tag{1}$$

where the strain invariants are:

$$J_1 = \text{Trace}[\mathbf{B}], \quad J_2 = \frac{J_1 - \text{Trace}[\mathbf{B}^2]}{2J_3},$$

$$J_3 = \sqrt{\det \mathbf{B}} = 1. \tag{2}$$

$\mathbf{B}$ is a left Cauchy–Green strain tensor. For infinitesimal strain conditions, the sum of constants C_{10} and C_{01} have a physical meaning of one-half of the shear modulus, i.e.

$$\tfrac{1}{2}\mu_0 = C_{10} + C_{01}. \tag{3}$$

The energy dependence on strain invariants only comes from the assumption that brain tissue is initially *isotropic*. The common assumption of tissue incompressibility results in the third strain invariant being equal to one. The first two terms in equation (1) form a well known Mooney–Rivlin energy function, originally developed for incompressible rubbers (for discussion see Rivlin, 1984).

In experiments conducted the deformation was orthogonal, and hence the left Cauchy–Green strain tensor had

only diagonal components:

$$\mathbf{B} = \begin{bmatrix} \lambda_z^2 & 0 & 0 \\ 0 & \lambda_z^{-1} & 0 \\ 0 & 0 & \lambda_z^{-1} \end{bmatrix}, \tag{4}$$

where λ_z is a stretch in vertical direction [Fig. 1(b)].

In such case, taking $J_1 = \lambda_z^2 + 2\lambda_z^{-1}$ and $J_2 = \lambda_z^{-2} + 2\lambda_z$, allows computation of the only non-zero Lagrange stress components from the simple formula

$$T_{zz} = \frac{\partial W}{\partial \lambda_z}. \tag{5}$$

Modelling of the loading velocity-dependent tissue behaviour

To model the time-dependent behaviour of the tissue the coefficients in the formula for energy function (1) can be written in the form of exponential series:

$$C_{ij} = C_{ij\infty} + \sum_{k=1}^{n} C_{ijk} e^{-t/\tau_k}, \tag{6}$$

and the energy function can be presented in the form of a convolution integral:

$$W = \int_0^t \left\{ \sum_{i+j=1}^{N} C_{ij}(t-\tau) \frac{\mathrm{d}}{\mathrm{d}\tau} [(J_1 - 3)^i (J_2 - 3)^j] \right\} \mathrm{d}\tau. \tag{7}$$

Substitution to equation (5) yields:

$$T_{zz} = \int_0^t \left\{ \sum_{i+j=1}^{N} C_{ij}(t-\tau) \frac{\mathrm{d}}{\mathrm{d}\tau} \left[\frac{\partial}{\partial \lambda_z} ((J_1 - 3)^i (J_2 - 3)^j) \right] \right\} \mathrm{d}\tau. \tag{8}$$

Equation (8) served as a basis for the comparison of the theory and experiment.

Determination of material constants for swine brain tissue

To obtain a good agreement between theory and experiment, it was necessary to retain second-order terms in the energy function (1). Then, for $N = 2$;

$$\begin{aligned} T_{zz} = \int_0^t \Big\{ & C_{10}(t-\tau) \frac{\mathrm{d}}{\mathrm{d}\tau} (2\lambda_z - 2\lambda_z^{-2}) \\ & + C_{01}(t-\tau) \frac{\mathrm{d}}{\mathrm{d}\tau} (-2\lambda_z^{-3}) \\ & + C_{11}(t-\tau) \frac{\mathrm{d}}{\mathrm{d}\tau} [(\lambda_z^2 + 2\lambda_z^{-1} - 3)(\lambda_z^{-2} + 2\lambda_z - 3)] \\ & + C_{20}(t-\tau)(\lambda_z^2 + 2\lambda_z^{-1} - 3) \frac{\mathrm{d}}{\mathrm{d}\tau} (2\lambda_z - 2\lambda_z^{-2}) \\ & + C_{02}(t-\tau)(\lambda_z^{-2} + 2\lambda_z - 3) \frac{\mathrm{d}}{\mathrm{d}\tau} (-2\lambda_z^{-3}) \Big\} \mathrm{d}\tau. \end{aligned} \tag{9}$$

In the case of the compression with constant velocity, the integral (9) can be evaluated analytically. The result obtained by application of *Mathematica* (Wolfram, 1996) is long and is not presented here. It is important to note, however, that the expression for stresses is linear in material parameters $C_{ij\infty}$ and C_{ijk}.

To accurately model the tissue behaviour for a wide range of loading velocities, it was necessary to use two time-dependent terms in the C_{ij} expansion [$n = 2$ in equation (6)]. This was dictated by the large span of the values of imposed strain rates and durations of experiments. It is not possible with only one exponentially decaying time-dependent term to reproduce the results having strain rates ranging over five orders of magnitude. To uniquely determine material coefficients $C_{ij\infty}$ and C_{ijk} [equation (6)] a few additional assumptions were adopted. The equality of the energy of reciprocal deformation to that of the original one (see Mooney, 1940) was assumed: $C_{01}/C_{10} = 1$ and $C_{02}/C_{20} = 1$. C_{11} was assumed to equal 0. Two time constants, $T_1 = 50$ (s); $T_2 = 0.5$ (s), were chosen to be approximately equal to the duration of the medium and fast tests, respectively. These assumptions left six constants to be determined.

The influence of the exponentially decaying terms on the results of the slow test is very small, so that during the procedure of determining equilibrium coefficients $C_{10\infty} = C_{01\infty}$, $C_{20\infty} = C_{02\infty}$, the remaining coefficients were set to zero. The function *Regress*, available in Mathematica software package (Wolfram Research 1996), was used to find least-squares fit to the slow test data. The result showed that the coefficients $C_{20\infty} = C_{02\infty}$ do not improve quality of fit and therefore they were set to zero.

Similar procedure, using the results of the medium speed tests and time constant τ_1, was applied to evaluate estimates for $C_{101} = C_{011}$ and $C_{201} = C_{021}$. Since the material constants associated with the characteristic time τ_2 have very little influence on the predictions for medium speed test (lasting about hundred times longer than the characteristic time τ_2) they were set to zero. Constants $C_{10\infty} = C_{01\infty}$, were set to the values obtained for the slow test, in the way described above.

Likewise, estimates of $C_{102} = C_{012}$ and $C_{202} = C_{022}$ were found, using fast tests results and time constant τ_2. The coefficients $C_{10\infty} = C_{01\infty}$, $C_{101} = C_{011}$ and $C_{201} = C_{021}$ were set to the values obtained using slow- and medium-speed test data. Table 1 contains the values of estimated material coefficients for brain tissue together with multiple correlation coefficients characterising the quality of fit.

Table 1. Brain material coefficients and multiple correlation coefficients

Equilibrium (slow-speed test results used)	Characteristic time $T_1 = 50$ (s) (medium-speed test results used)	Characteristic time $T_2 = 0.5$ (s) (fast-speed test results used)
$C_{10\infty} = C_{01\infty} = 81$ (Pa); $R^2 = 0.9975$ $C_{20\infty} = C_{02\infty} = 0$	$C_{101} = C_{011} = 26$ (Pa); $R^2 = 0.9945$ $C_{201} = C_{021} = 395$ (Pa); $R^2 = 0.9945$	$C_{102} = C_{012} = 163$ (Pa); $R^2 = 0.9673$ $C_{202} = C_{022} = 84$ (Pa); $R^2 = 0.9673$

Because of the variance dependence on strain (Fig. 3), standard methods, such as the t-test, could not be used to determine the confidence intervals for regression coefficients.

DISCUSSION AND CONCLUSIONS

In this study, the results of *in vitro* unconfined compression of swine brain tissue and the mathematical model of tissue deformation behaviour are presented.

Non-linear stress–strain relations were observed. A strong dependence between stresses and strain rate was recorded. Since previously reported experiments (Estes and MacElhaney, 1970; Galford and MacElhaney, 1970) were designed to simulate brain tissue behaviour under the conditions of a car accident or other impacts, applied strain rates were orders of magnitude higher than those in this study, and compressive strains reached about 0.9. The experiments conducted in this work were designed to give more insight into the tissue behaviour at lower compressive strains and strain rates, which are typical for surgical procedures.

The use of the single-phase, non-linear, viscoelastic model based on the concept of the strain energy function, in the form of convolution integral with coefficient expressed in the form of exponential series, is described. Agreement between the proposed theoretical model and experiment is good for compression levels reaching 30% and for loading velocities varying over five orders of magnitude.

Recently, Mendis *et al.* (1995) employed a similar modelling method. In our opinion, however, the results reported in their paper may be misleading. Serious reservation arises with regard to the determination of quasi-static parameters of Mooney–Rivlin strain energy function. Mendis *et al.* assume that the results of the tests presented in Estes and McElhaney (1970), for the smallest loading velocity can be regarded as quasi-static. Results obtained in this work indicate that this assumption is incorrect. The slowest unconfined compression tests reported in Estes and McElhaney (1970) used the indentor velocity of 0.508 mm s^{-1}, which corresponds to the strain rate of approximately $-0.1\ s^{-1}$ (under assumption that the sample height was 0.2 in = 5.08 mm). Experimental data presented here (Fig. 3) indicate that the estimation of quasi-static material constants requires much slower tests. The compressive forces in the experiments conducted with indentor speed of 5 mm min^{-1}, corresponding to the strain rate of $0.64 \times 10^{-2}\ s^{-1}$ (smaller than the one of the slowest test reported in Estes and McElhaney, 1970) are much larger than in slowest test presented in this work (Fig. 3). Though not ideal, the experimental data reported here could serve to determine better the static (or quasi-static) properties of the brain tissue, than those obtained by Estes and McElhaney.

The specimens used in the experiments consisted of the arachnoid membrane, white matter and grey matter. Subsequently, the criticism may arise that the experimental results are only valid for such a composite. However, we think that our results are still useful in approximate modelling the behaviour of the brain tissue, which includes spatial averaging of material properties. Furthermore, the average properties of the specimen consisting of white and grey matter, and arachnoid membrane are meaningful in the clinical situations. In the case of brain surgery, the sulcus is pushed aside to access lesions. To avoid damage to the brain, neurosurgeons try not to destroy the arachnoid membrane.

One advantage of the model proposed is that the constitutive equation developed here is already available in ABAQUS Finite Element Method Software Package (ABAQUS, 1992) and can be used immediately for larger-scale computations.

How to use the *in vitro* experimental results in the more realistic *in vivo* environment remains an open question. More experimental work is required to verify the validity of the assumptions used for model derivation as well as the numerical values of brain tissue material constants. Further research is needed to determine brain tissue constitutive models, which would incorporate the influence of the blood and cerebrospinal fluid pressure and flow.

Acknowledgements—The authors would like to thank most sincerely all the members of Biomechanics Division of Mechanical Engineering Laboratory, MITI and Dr Tetsuya Tateishi not forgetting Mr Yoshio Shirasaki and Mr Kazuya Machida, for their indispensable help. We thank Dr Mark L. Ford and Miss Helen L. Clarke for careful reading of the manuscript. The financial support of Japanese Science and Technology Agency and the New Energy and Industrial Technology Development Organisation (NEDO) is gratefully acknowledged.

REFERENCES

ABAQUS Theory Manual (1992) Version 5.2, Hibbit, Karlsson and Sorensen, Inc.

Borowski, S., Dietrich, M., Kedzior, K., Kurowski, P., Matyjewski, M., Miller K., Rzymkowski, C., Walczak, Z. and Zagrajek, T. (1992) Modeling and simulation of human musculoskeletal system. In *Proceedings of the 6th Biomechanics Seminar*, eds C. Hogfors and G. Andreasson, pp. 116–134. Center for Biomechanics, Chalmers University of Technology, Sweden.

Brett, P. N., Fraser, C. A., Henningan, M., Griffiths, M. V. and Kamel Y. (1995) Automatic surgical tools for penetrating flexible tissues. *IEEE Engineering and Medical Biology* 264–270.

Burdea, G. (1996) *Force and Touch Feedback for Virtual Reality*. Wiley, New York.

Estes, M. S. and McElhaney J. H. (1970) Response of brain tissue of compressive loading. ASME Paper No. 70-BHF-13.

Fung Y. C. (1981) *Biomechanics. Mechanical Properties of Living Tissues*. Springer, New York.

Galford, J. E. and McElhaney, J. H. (1970) A viscoelastic study of scalp, brain and dura. *Journal of Biomechanics* **3**, 211–221.

Gallagher, R. H., Simon, B. R., Johnson, P. C. and Gross, J. F. (eds) (1982) *Finite Elements in Biomechanics*. Wiley, New York.

Kumagaya, T. and Namioka, S. (eds) (1987) *Hyology and Hyoiatrics*. Kindai Press, Tokyo (in Japanese).

Lavallée, S. (1995) Registration for computer integrated surgery: methodology, state of the art. In *Computer-Integrated Surgery*, pp. 77–97, MIT Press, Cambridge, MA.

Mendis, K. K., Stalnaker, R. L. and Advani S. H. (1995) A constitutive relationship for large deformation finite element modeling of brain tissue. *Trans. ASME Journal of Biomechanical Engineering* **117**, 279–285.

Miller, K. and Chinzei, K. (1995a) Modeling of soft tissues. *Mechanical Engineering Laboratory News* **12**, 5–7 (in Japanese).

Miller, K. and Chinzei, K. (1995b) Modeling of soft tissues deformation. *Journal of Computer Aided Surgery* **1** (*Suppl.*); *Proceedings of the 2nd International Symposium on Computer Aided Surgery*, Tokyo Women's Medical College, Shinjuku, Tokyo, pp. 62–63.

Mooney, M. (1940) A theory of large elastic deformation. *Journal of Applied Physics* **11**, 582–592.

Mow, V. C., Ateshian, G. A. and Spilker R. L. (1993) Biomechanics of diarthrodial joints: a review of twenty years of progress. *Trans. ASME Journal of Biomechanical Engineering* **115,** 460–467.

Ommaya, A. K. (1968) Mechanical properties of tissues of the nervous system. *Journal of Biomechanics* **1,** 127–138.

Pamidi, M. R. and Advani, S. H. (1978) Nonlinear Constitutive Relations for Human Brain Tissue. *Trans. ASME Journal of Biomechanics Engineering* **100,** 44–48.

Rivlin, R. S. (1984) Forty Years of nonlinear continuum mechanics. *Proceedings of the IX International Congress on Rheology*, Mexico, pp. 1–29.

Ruan, J. S., Khalil, T. and King A. I. (1994) Dynamic response of the human head to impact by three-dimensional finite element analysis. *Trans. ASME Journal of Biomechanical Engineering* **116,** 44–50.

Sahay, K. B., Mehrotra, R., Sachdeva, U. and Banerji, A. K. (1992) Elastomechanical characterization of brain tissues. *Journal of Biomechanics* **25,** 319–326.

Schmid-Schonbein, G. W., Woo, S. L-Y. and Zweifach, B. W. (eds) (1986) *Frontiers in Biomechanics*. Springer, New York.

Voo, L., Kumaresan, S., Pintar, F. A., Yoganandan, N. and Sances, Jr, A. (1996) Finite-element models of the human head. *Medical and Biological Engineering Computation* **34,** 375–381.

Walsh, E. K. and Schettini, A. (1984) Calculation of brain elastic parameters *in vivo*. *American Journal of Physiology* **247,** R637–R700.

Wolfram, S. (1996) *Mathematica Book*, 3rd Edn *Wolfram Media*, pp. 816–820. Cambridge University Press, U.S.A.

Wolfram Research (1996) *Mathematica 3.0 Standard Add-on Packages*, *Wolfram Media*, pp. 428–439. Cambridge University Press, U.S.A.